ACCSCIENCE PUBLISHING

Advanced Neurology

ORIGINAL RESEARCH ARTICLE

Decreased cortical thickness and normal regional homogeneity underlying cognitive impairment in cerebral small vessel disease

Yuting Mo[1,2,3†], Lili Huang[1,2,3†], Ruomeng Qin[1,2,3], Kelei He[4], Zhihong Ke[1,2,3], Zheqi Hu[1,2,3], Chenglu Mao[1,2,3], Biyun Xu[5], Ruowen Qi[5], Xiaolei Zhu[1,2,3*], and Qing Ye[1,2,3*]

[1]Department of Neurology of Drum Tower Hospital, Medical School and the State Key Laboratory of Pharmaceutical Biotechnology, Nanjing University, Nanjing 210008, China

[2]Nanjing Neurology Clinic Medical Center, Nanjing 210008, China

[3]Institute of Brain Science, Nanjing University, Nanjing 210008, China

[4]National Institute of Healthcare Data Science at Nanjing University, China

[5]Medical Statistics and Analysis Center, Nanjing Drum Tower Hospital, Nanjing University Medical School, 321 Zhongshan Road, Nanjing, 210008, China

Abstract

Cerebral small vessel disease (CSVD) is the most common cause of vascular cognitive impairment (CI). However, the cognitive performance of individuals with CSVD varies considerably. Early identification of neuroimaging changes related to CI caused by CSVD is important for the prediction and management of CI. The present study aimed to explore the early alterations in cortical thickness and regional homogeneity (ReHo) related to CI in people with CSVD. A total of 106 participants with CSVD with CI, 77 participants with CSVD without CI, and 121 control participants underwent neuropsychological tests and multimodal magnetic resonance imaging scans. Cortical thickness was analyzed using FreeSurfer software, and ReHo patterns were explored using the DPARSF toolbox in brain regions that exhibited alterations in cortical thickness. The CSVD with CI group exhibited decreased cortical thickness but normal ReHo in the right anterior cingulate gyrus (ACG), right cuneus, bilateral insula, and right middle temporal gyrus compared with that in the other two groups. Specifically, both cortical thickness and ReHo in the right ACG were significantly associated with memory performance in CSVD patients with CI. In addition, impaired visuospatial function occurred earlier than the decline of global function in CSVD patients and was related to cortical thinning in the right middle temporal gyrus. In conclusion, decreased cortical thickness but normal ReHo in the right ACG, right cuneus, bilateral insula, and right middle temporal gyrus are characteristic alterations related to the development of CI in CSVD patients. These findings may contribute to the early prediction of CI in CSVD patients.

Keywords: Cerebral small vessel disease; Cognitive impairment; Cortical thickness; Regional homogeneity

†These authors contributed equally to this work

***Corresponding authors:**
Qing Ye (yeqingyouxiang@126.com)
Xiaolei Zhu (zhuquelee@126.com)

Citation: Mo Y, Huang L, Qin R, *et al*., 2022, Decreased cortical thickness and normal regional homogeneity underlying cognitive impairment in cerebral small vessel disease. *Adv Neuro*, 1(1): 48. https://doi.org/10.36922/an.v1i1.48

Received: November 16, 2021

Accepted: March 14, 2022

Published Online: March 30, 2022

1. Introduction

Cerebral small vessel disease (CSVD) is a clinical syndrome involving injuries in small vessels in the brain and typically causes cognitive impairment (CI), gait dysfunction, and mood disorders, as well as urinary and rectal dysfunction. The common neuroimaging features of CSVD include white matter (WM) hyperintensities (WMH), lacunes, microbleeds, and perivascular space enlargement[1]. CSVD is an age-related disease detected in more than 68% of people over 60 years old and is the most common cause of vascular CI, contributing to 45% of dementia cases[2]. However, the cognitive performance of individuals with CSVD tends to vary markedly, with a proportion of these individuals exhibiting normal cognitive function[3]. Exploring the brain alterations related to the development of CI in CSVD patients is essential for the prediction and management of CI in these patients.

Recently, multimodal functional magnetic resonance imaging (fMRI) has been used to detect functional and structural brain alterations related to CI in CSVD patients. For example, altered patterns of resting-state networks, including the default mode network, the frontoparietal control network, and the dorsal attention network, are associated with CI in CSVD patients[4-6]. The impaired information processing speed caused by CSVD is mediated by the nodal global efficiency of resting-state functional networks in the frontal and parietal regions[7]. Fiber microstructural integrity, which can be measured using diffusion tensor imaging technology, is also associated with cognitive performance in CSVD patients. Fiber integrities in the cingulum bundle, the frontal WM, and the corpus callosum are related to verbal memory, psychomotor speed, and global cognitive function, respectively[8]. However, the methodologies used for exploring resting-state networks and fiber microstructural integrity vary across studies, and it is time consuming to perform analyses of resting-state networks and fiber microstructural integrity. These factors limit the clinical application of these methodologies for predicting the development of CI in CSVD patients.

Cortical thickness is a reliable parameter for assessing structural atrophy in the cerebral cortex. CSVD patients are reported to exhibit cortical thinning in several brain regions, including the bilateral temporal lobe, and bilateral insula[9-11]. However, the patterns of cortical thinning related to the CI caused by CSVD vary across studies[12]. This variation may have been caused by heterogeneity in methodologies, including the definition of CI, the calculation of cortical thickness, and insufficient sample size. As a result, the pattern of cortical thinning related to the development of CI in CSVD patients remains relatively poorly understood. In addition, cortical atrophy may be associated with altered regional functional homogeneity in the cortex. Regional homogeneity (ReHo), a widely used functional homogeneity parameter, measures the consistency of a time series of a given voxel with its neighboring voxels using Kendall's coefficient concordance and indicates the synchronized oscillation of neurons in a given brain region[13]. Our recent study revealed that CSVD patients with CI exhibited higher ReHo in parietal and occipital regions than CSVD patients without CI[14]. However, determining whether there is a connection between altered ReHo and cortical atrophy requires further investigation. Exploring the patterns of cortical thinning and ReHo in CSVD patients with and without CI may be useful for the prediction of CI in these patients.

In the present study, participants exhibiting CSVD with CI, participants exhibiting CSVD without CI, and normal control (NC) participants underwent neuropsychological testing and multimodal fMRI scans. We aimed to: (1) Explore the different patterns of cortical thinning and ReHo across groups and (2) detect early alterations in cortical thickness and ReHo related to the development of CI in CSVD patients.

2. Methods

2.1. Participants

A total of 183 CSVD patients and 121 NC participants were recruited at the Affiliated Drum Tower Hospital of Nanjing University Medical School. This study was approved by the Affiliated Drum Tower Hospital of Nanjing University Medical School Ethics Committee and written informed consent was obtained from each participant. All participants underwent multimodal MRI scans and standardized clinical assessments, including demographic data, vascular risk factor recording, and neuropsychological examination. The inclusion criteria for CSVD patients were as follows: (1) Age between 50 and 80 years; (2) meeting the diagnostic criteria for CSVD; (3) right handed; and (4) no contraindications for MRI.

The diagnosis of CSVD was based on neuroimaging and clinical symptoms. On the basis of established research criteria, the detailed diagnostic criteria are as follows: (1) Lesions of moderate-to-severe WMH[15] (Fazekas scores of 2 or higher) and/or anatomically appropriate lacunar infarcts on neuroimaging, with or without perivascular spaces, microbleeds, and brain atrophy[16,17] and (2) acute symptoms (e.g., lacunar syndromes and transient ischemic attack) or subacute manifestations (e.g., CI, motor disturbances, and emotional disorders).

The exclusion criteria were as follows: (1) A history of ischemic stroke with infarct size more than 1.5 cm in

diameter; (2) cerebral hemorrhage; (3) internal carotid artery or vertebral artery stenosis (>50%) or coronary atherosclerosis heart disease; (4) other neurological disorders, such as Alzheimer's disease (AD), Parkinson's disease, epilepsy, or mental disorders; (6) serious physical illnesses, such as cancer; and (7) any conditions that interfere with cognitive examination, such as blindness, deafness-muteness, or physical disability.

The inclusion criteria for the NC group were as follows: (1) Age between 50 and 80 years; (2) no clinical symptoms of CSVD or MRI presentative characteristics of CSVD; and (3) normal cognitive function.

The Montreal Cognitive Assessment (MoCA) test was used to define whether the participants had CI. The education-adjusted cutoff values for the MoCA were ≤19 for 1–6 years of education, ≤24 for 7–12 years of education, and <26 for >12 years of education[18]. Participants with MoCA scores lower than education-adjusted norms were classified as having CI. According to MoCA scores, CSVD patients were divided into two groups, the CSVD-CI group (n = 106) and the CSVD-no-CI group (n = 77).

2.2. Clinical assessments

All participants underwent the same standardized neuropsychological test protocols, including the Hamilton Depression Rating Scale (HAMD) which evaluates depression, Hamilton Anxiety Rating Scale (HAMA) which evaluates anxiety, MoCA (Beijing version August 26, 2006, translated by Wang and Xie, www.mocatest.org), Auditory Verbal Learning Test (AVLT), Digit Span Test (DST), Boston Naming Test (BNT), and Stroop Color Word Test (SCWT). The AVLT, DST, BNT, and SCWT were used to conduct a detailed cognitive assessment involving multiple cognitive domains. The AVLT is a widely used test of verbal memory and contains three main indicators: AVLT immediate recall (AVLTIR), AVLT-short time delay recall (AVLTSTDR), and AVLT-long time delay recall (AVLTLTDR). The DST is a simple method for evaluating working memory, executive function, and attention. There are two parts in the DST: DST-forward (DSF) and DST-backward (DSB). To conduct a more comprehensive memory evaluation, the Wechsler Memory Scale-Visual Reproduction (VR) was also conducted for visual memory assessment and the scores of VR-Copy (VRC), VR-Immediate Recall (VRIR), and VR-Delayed Recall (VRDR) were statistically analyzed. The congruent part of the SCWT was used to evaluate processing speed, and the incongruent part of SCWT was used to assess executive function.

2.3. MRI data acquisition

The MRI scanning was conducted at the Affiliated Drum Tower Hospital of Nanjing University Medical School with a Philips 3.0-T scanner (Philips Medical Systems, Netherlands). The multimodal MRI scans included: (1) The high-resolution T1-weighted turbo gradient echo sequence, with repetition time (TR) = 9.8 ms, flip angle (FA) = 8°, echo time (TE) = 4.6 ms, field of view (FOV) = 250 mm × 250 mm, number of slices = 192, acquisition matrix = 256 × 256, and thickness = 1.0 mm, (2) the FLAIR sequence, with TR = 4500 ms, TE = 333 ms, time interval (TI) = 1600 ms, number of slices = 200, voxel size = 0.95 mm × 0.95 mm × 0.95 mm, and acquisition matrix = 270 × 260, and (3) the blood oxygen level dependent (BOLD) sequence, with TR = 2000 ms, TE = 30 ms, number of slices = 35, voxel size = 3.00 mm × 3.00 mm × 4.00 mm, and acquisition matrix = 64 × 62.

2.4. Structural MRI data

2.4.1. Preprocessing of T1-weighted MRI

FreeSurfer (version 6.0 for Linux)[19] was used to process the T1-weighted MRI scans. The detailed steps included: (1) Automated Talairach transformation, (2) subcortical segmentation of the WM and the deep gray matter (GM) volumetric structures, (3) intensity normalization[20], (4) segmentation of the brain tissue, including GM, WM, and cerebrospinal fluid (CSF), (5) surface modeling for the GM/WM and GM/CSF borders[21,22], (6) surface inflation[23], (7) registration to a spherical atlas that utilized individual cortical folding patterns to match cortical geometry across participants[24], (8) ROI establishment of the cerebral cortex on the basis of gyral and sulcal structure[25,26], and (9) cortical thickness calculation. Both intensity and continuity information of the whole 3D MR image volumes in the segmentation and deformation procedures were used during the process to produce representations of cortical thickness. At each vertex, the cortical thickness was calculated as the closest distance from the inner surface to the outer surface[27]. The Desikan–Killiany (DK) atlas was chosen for consistent brain measurements[28], because the boundaries it contains were suitable for the FreeSurfer classifier.

2.4.2. Cortical thickness analysis

Glmfit (analytic software in FreeSurfer) was used to analyze the whole-brain vertex-wise surface-based cortical thickness. To improve the signal-to-noise ratio, a 10 mm full width half maximum (FWHM) Gaussian spatial smoothing kernel was performed before analysis. A different offset same slope method was used to build a general linear model (GLM), which was a built-in analysis method in glmfit. Because of the variability in participants' demographic characteristics (sex, age, and years of education) served as the covariances for the GLM analysis. Multiple comparison corrections were performed using

Monte Carlo simulation correction with a vertex-wise/cluster-forming threshold of 3 ($P < 0.001$) and a cluster-wise $P < 0.001$ (two tailed). The cortical thicknesses of significant brain regions were extracted for further study.

2.5. fMRI data

2.5.1. Preprocessing of fMRI

The fMRI analysis was based on the BOLD sequence. DPARSF, a method based on the Resting-State Functional MR Imaging Toolkit (http://www.restfmri.net) and statistical parametric mapping software package (SPM12; www.fil.ion.ucl.ac.uk/spm), was used for the preprocessing of fMRI data. The preprocessing steps included removing the first 10 volumes of data, slice timing correction, realignment, reorientation, head motion correction (note that participants with head motion more than 2.0 mm of displacement in any direction, or 2.0° of rotation in any angular dimension were excluded), image segmentation for the high-resolution T1-weighted turbo gradient echo sequence and the BOLD sequence by Diffeomorphic Anatomical Registration Through Exponentiated Lie algebra, coregistration of T1 images to the functional images, normalization using a 12-parameter non-linear transformation to the standard Montreal Neurological Institute (MNI) space ($3 \times 3 \times 3$ mm^3), and band-pass filtering (0.01–0.08 Hz).

2.5.2. ReHo analysis

The purpose of the fMRI analysis was to explore the functional changes of certain brain regions that were extracted from the structural analysis. The significant brain regions in cortical thickness analysis were transferred into MNI space and defined as regions of interest (ROIs) in ReHo analysis. The ReHo analysis using the preprocessed fMRI data was also performed by DPARSF. The steps for acquiring the ReHo value after z-translation and smoothing were as follows: (1) Calculating the ReHo value of 27 voxels and doing a Z-transform, (2) smoothing the ReHo map after Z-transform with a Gaussian kernel of 6 mm FWHM for noise reduction, and (3) extracting ReHo values of the ROIs for further statistical analysis.

2.6. Statistical analysis

The demographic data were analyzed using SPSS 16.0 (SPSS, Chicago, IL, USA). All of the continuous variables were tested for normality before comparison. Analysis of variance (ANOVA) and the Kruskal–Wallis test were used to compare the variation in age, education, and cognitive scale scores among the three groups according to normality. A Chi-squared test was used for the comparison of sex and vascular risk factors among groups. Changes in ReHo across groups were analyzed using the GLM, controlling for differences in age and education. Bonferroni correction was applied in the GLM for *post hoc* multiple comparison corrections. Partial correlation analysis was conducted to explore the relationships between MRI parameters and cognitive scale scores, with age and education as covariates. $P < 0.05$ was considered to indicate statistical significance.

3. Results

3.1. Clinical assessments

Demographically, there was no difference in sex among the CSVD-CI group, CSVD-no-CI group, and NC group. However, both of the CSVD groups were older than the NC group, and the CSVD-CI group had fewer years of education than the other two groups. There was no significant difference in Fazekas scores, lacunar infarcts count, and microbleeds between the CSVD-CI group and the CSVD-no-CI group. In terms of vascular risk factors, there was a significant difference in hypertension, but no significant differences in diabetes, hyperlipidemia, and smoking. In neuropsychological evaluation, there were significant differences in HAMD and VRIR scores between the CSVD-no-CI group and the NC group. *Post hoc* multiple comparisons were performed among the CSVD-CI group, CSVD-no-CI group, and NC group. Detailed information regarding the clinical assessments is shown in Tables 1-3.

3.2. Cortical thickness analysis

There were significant differences in cortical thickness among the CSVD-CI group, CSVD-no-CI group, and NC group in the left insula, right insula, right anterior cingulate gyrus (ACG), right cuneus, and right middle temporal gyrus (MTG). *Post hoc* multiple comparisons were performed among the CSVD-CI group, CSVD-no-CI group, and NC group, adding age and education as covariates. Detailed information for the cortical thickness analysis is shown in Figure 1, Tables 4 and 5. The CSVD-CI group exhibited lower cortical thickness in all five regions compared with that in the other two groups, and the CSVD-no-CI group exhibited lower cortical thickness only in the bilateral insula and the right MTG compared with that in the NC group.

3.3. ReHo analysis

The five brain regions exhibiting group differences in cortical thickness analysis were targeted as the ROIs in ReHo analysis. ReHo values of ROIs were extracted, followed by GLM analysis (adding age and education as covariates, using Bonferroni correction for *post hoc* multiple comparisons). There were significant differences in ReHo values of the left insula ($P = 0.005$) and right insula ($P = 0.024$) among the CSVD-CI group, CSVD-

Table 1. Details of missing data

	CSVD-CI group (*n*=106) *n* (missing)	CSVD-no-CI group (*n*=77) *n* (missing)	NC group (*n*=121) *n* (missing)
T1-weighted MRI	106 (0)	77 (0)	121 (0)
fMRI	94 (12)	70 (7)	106 (15)
Neuroimaging features	106 (0)	77 (0)	121 (0)
Sex	106 (0)	77 (0)	121 (0)
Age	104 (2)	76 (1)	120 (1)
Education	106 (0)	76 (1)	121 (0)
Vascular risk factors	106 (0)	77 (0)	121 (0)
HAMD	100 (6)	71 (6)	114 (7)
HAMA	99 (7)	71 (6)	114 (7)
MoCA	106 (0)	77 (0)	121 (0)
VRC	80 (26)	59 (18)	100 (21)
VRIR	81 (25)	59 (18)	99 (22)
VRDR	81 (25)	59 (18)	100 (21)
AVLTIR	81 (25)	59 (18)	100 (21)
AVLTSTDR	79 (27)	55 (22)	96 (25)
AVLTLTDR	78 (28)	55 (22)	97 (24)
DSF	94 (12)	65 (12)	110 (11)
DSB	93 (13)	65 (12)	110 (11)
SCWT – congruent part	88 (18)	66 (11)	109 (12)
SCWT – incongruent part	90 (16)	66 (11)	109 (12)
BNT	81 (25)	58 (19)	100 (21)

no-CI group, and NC group. Detailed information of ReHo analysis is shown in Table 6. Specifically, the CSVD-no-CI group had lower ReHo in the two regions compared with the NC group, whereas no significant difference was found between the CSVD-CI group and the NC group, or between the two CSVD groups.

3.4. Correlation analysis

We assessed the relevance of the MRI parameters to cognitive scale scores while adjusting for age and education as covariates. In the NC group, no clinically significant correlations were found. In the CSVD-CI group, cortical thickness of the right ACG showed a significant positive relationship with DSF scores (r = 0.339, P = 0.001). The ReHo values in the right ACG were negatively correlated with AVLT scores (AVLTIR: r = −0.369, P = 0.002; AVLTSTDR: r = −0.356, P = 0.003; and AVLTLTDR: r = −0.372, P = 0.002) in the CSVD-CI group. However, in the CSVD-no-CI group, the correlations mentioned above were not observed. Cortical thickness of the right MTG in the CSVD-no-CI group was positively correlated with BNT scores (r = 0.327, P = 0.015) and VR scores (VRC: r = 0.353, P = 0.008; VRIR: r = 0.398, P = 0.002; and VRDR: r = 0.305, P = 0.022) (Table 7).

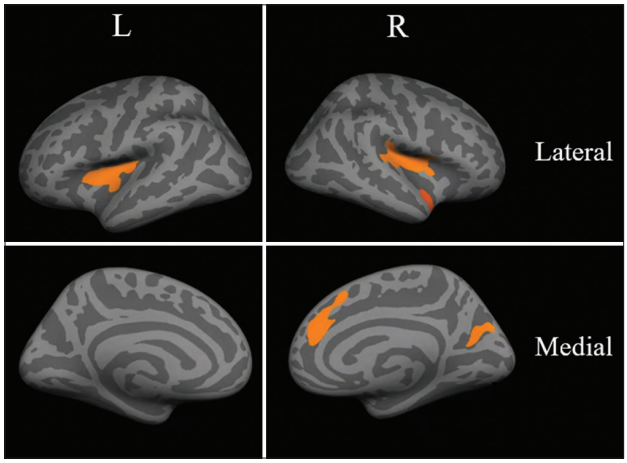

Figure 1. The color-shaded areas correspond to the bilateral insula, right ACG, right cuneus, and right middle temporal gyrus, where significant differences were found in cortical thickness analysis. L, left cerebral hemisphere; R, right cerebral hemisphere.

4. Discussion

This study explored the cortical thickness and ReHo patterns in CSVD patients with and without CI. The results revealed that (1) CSVD patients with CI displayed decreased cortical thickness but normal ReHo in the right ACG, right cuneus, bilateral insula, and right MTG; (2) both the cortical thickness and ReHo in the right ACG were significantly associated with the memory performance of CSVD patients with CI; and (3) impaired visuospatial function occurred earlier than the decline in global function in CSVD patients and was associated with cortical thinning in the right MTG.

Although the CSVD with CI group and the CSVD without CI group had comparable burdens in WMH, cerebral microbleeding, and lacunar infarction, the two groups showed distinct differences in cognitive performance. This suggests that the conventional imaging burden of CSVD is not strongly associated with cognitive performance of CSVD patients. The previous studies reported that the WMH burden was not associated or was only mildly associated with cognitive performance[15,29,30]. Some previous studies reported a link between cerebral microbleeding and cognitive performance, whereas others did not[31,32]. The same is true for the association of lacunar infarction with cognitive function[33]. In contrast, our findings revealed that cortical thinning was related to the cognitive performance of CSVD patients. These findings may contribute to the explanation of markers that can predict the onset of CI in these patients.

Table 2. Results of clinical assessments

	CSVD-CI group (*n*=106)	CSVD-no-CI group (*n*=77)	NC group (*n*=121)	Statistics	*P*-value
Demographics					
Sex					
Male	61 (57.55)	48 (62.34)	67 (55.37)	0.945	0.624[a]
Female	45 (42.45)	29 (37.66)	54 (44.63)		
Age (years, mean±s.d.)	66.00±8.25	65.68±9.45	60.52±7.76	14.686	<0.001[b]
Education (years) [d]	9.00 (9.00–12.00)	12.00 (9.00–15.00)	12.00 (9.00–15.00)	7.531	0.023[c]
Vascular risk factors					
Hypertension, n (%)	64 (60.38)	56 (72.73)	64 (52.89)	7.750	0.021[a]
Diabetes, n (%)	21 (19.81)	23 (29.87)	21 (17.36)	4.623	0.099[a]
Hyperlipidemia, n (%)	23 (21.70)	16 (20.78)	23 (19.01)	0.261	0.878[a]
Smoking, n (%)	16 (15.09)	14 (18.18)	16 (13.22)	0.901	0.637[a]
Fazekas scores[d]	2.00 (2.00–3.00)	2.00 (2.00–3.00)	1.00 (1.00–1.00)	157.302	<0.001[c]
Lacunar infarcts count[d]	2.00 (1.00–4.25)	1.00 (0.00–3.50)	0.00 (0.00–0.00)	148.070	<0.001[c]
Microbleeds[d]	1.00 (0.00–3.00)	1.00 (0.00–3.00)	0.00 (0.00–0.00)	66.865	<0.001[c]
Neuropsychological data					
HAMD[d]	6.00 (3.00–9.00)	3.00 (1.00–7.00)	5.00 (2.00–9.00)	9.294	0.010[c]
HAMA[d]	7.00 (3.00–12.00)	5.00 (1.00–11.00)	6.00 (3.00–13.25)	3.072	0.215[c]
MoCA[d]	21.00 (18.00–23.00)	26.00 (25.00–27.00)	27.00 (25.00–28.00)	154.356	<0.001[c]
VRC[d]	14.00 (13.00–14.00)	14.00 (14.00–14.00)	14.00 (14.00–14.00)	13.999	0.001[c]
VRIR[d]	8.00 (5.00–10.00)	10.00 (7.00–12.00)	11.00 (9.00–13.00)	38.384	<0.001[c]
VRDR[d]	5.00 (3.00–9.00)	8.00 (5.00–11.00)	9.50 (6.00–12.00)	22.957	<0.001[c]
AVLTIR[d]	12.00 (10.00–16.00)	15.00 (13.00–18.00)	17.00 (14.00–20.00)	35.777	<0.001[c]
AVLTSTDR (mean±s.d.)	3.44±2.37	5.15±2.38	5.71±2.11	22.467	<0.001[b]
AVLTLTDR (mean±s.d.)	3.06±2.17	5.00±2.18	5.38±2.16	26.622	<0.001[b]
DSF[d]	8.00 (7.00–8.00)	8.00 (7.50–9.00)	8.00 (8.00–9.00)	15.176	0.001[c]
DSB[d]	4.00 (3.00–5.00)	5.00 (4.00–6.00)	5.00 (4.00–6.00)	19.107	<0.001[c]
SCWT – congruent part[d]	23.50 (18.00–30.25)	16.00 (14.00–22.00)	17.00 (14.00–20.50)	45.707	<0.001[c]
SCWT – incongruent part[d]	12.00 (4.25–20.00)	11.00 (5.00–20.25)	11.00 (5.50–17.00)	0.380	0.827[c]
BNT[d]	48.00 (40.00–52.50)	52.00 (48.00–55.25)	54.00 (49.25–56.75)	29.620	<0.001[c]

s.d.: Standard deviation, [a]: *P* value of Chi-squared test, [b]: *P* value of ANOVA, [c]: *P* value of Kruskal–Wallis test, [d]: Data with non-normal distribution were described by median (interquartile range)

In general, the CSVD with CI group displayed decreased cortical thickness in five regions, including the right ACG, right cuneus, bilateral insula, and right MTG, whereas the CSVD without CI group only exhibited decreased cortical thickness in the latter three regions. This suggests that cortical thinning in bilateral insula and right MTG is related to the development of CSVD, and cortical thinning in the right ACG and right cuneus is related to the development of CI in these patients. Similarly, cortical thinning in the bilateral insula, right cuneus, and right MTG has been reported in subcortical ischemic vascular disease patients and patients with CI showed more extensive cortical thinning than those without CI[34]. In the present study, the contribution of cortical thinning in the right ACG to CI in CSVD patients has been reported for the 1st time.

In addition, the ReHo analysis showed that the CSVD without CI group exhibited decreased ReHo values in bilateral insula, whereas the CSVD with CI group showed no changes in ReHo values compared with the NC group. One previous study revealed no significant difference in ReHo between patients with lacunar infarctions and mild CI and NC participants[35]. On the basis of the present findings, we speculate that cortical thinning in the five

Table 3. *P* values of *post hoc* multiple comparisons in clinical assessments among the CSVD-CI group, CSVD-no-CI group, and NC group

	Between CSVD-CI group and NC group	Between CSVD-CI group and CSVD-no-CI group	Between CSVD-no-CI group and NC group
Age	<0.001[a]	0.803[a]	<0.001[a]
Education	0.026[b]	0.012[b]	0.821[b]
Fazekas scores	<0.001[b]	0.688[b]	<0.001[b]
Lacunar infarcts count	<0.001[b]	0.166[b]	<0.001[b]
Microbleeds	<0.001[b]	0.307[b]	<0.001[b]
HAMD	0.385[b]	0.003[b]	0.024[b]
HAMA	0.947[b]	0.103[b]	0.133[b]
MoCA	<0.001[b]	<0.001[b]	0.524[b]
VRC	<0.001[b]	0.035[b]	0.481[b]
VRIR	<0.001[b]	0.001[b]	0.017[b]
VRDR	<0.001[b]	0.006[b]	0.184[b]
AVLTIR	<0.001[b]	<0.001[b]	0.052[b]
AVLTSTDR	<0.001[a]	<0.001[a]	0.144[a]
AVLTLTDR	<0.001[a]	<0.001[a]	0.298[a]
DSF	<0.001[b]	0.003[b]	0.965[b]
DSB	<0.001[b]	0.003[b]	0.531[b]
SCWT - congruent part	<0.001[b]	<0.001[b]	0.742[b]
SCWT - incongruent part	0.647[b]	0.882[b]	0.575[b]
BNT	<0.001[b]	<0.001[b]	0.193[b]

[a]: *P* value of *post hoc* multiple comparisons in ANOVA, [b]: *P* value of *post hoc* multiple comparisons in Kruskal–Wallis test

Table 4. Regions showing significant differences in cortical thickness in the CSVD-CI group, CSVD-no-CI group, and NC group

Brain region	Side	MNI coordinate			Cluster size (mm^2)	CSVD-CI group versus NC group [a]	CSVD-CI group versus CSVD-no-CI group[a]	NC group versus CSVD-no-CI group[a]
		x	y	Z				
Insula	Left	−35.4	−6.0	10.6	1066.79	<0.001	<0.001	0.007
Insula	Right	34.8	−15.8	18.2	1064.36	<0.001	0.002	<0.001
ACG	Right	9.5	36.8	30.0	682.55	<0.001	<0.001	1.000
Cuneus	Right	22.7	−64.2	23.5	446.76	<0.001	<0.001	1.000
MTG	Right	48.1	0.1	−17.9	332.47	<0.001	0.040	0.007

Notes: General linear model adjusted for sex, age, and education was used for cortical thickness analysis in FreeSurfer among the CSVD-CI group, CSVD-no-CI group, and NC group. Monte Carlo simulation correction was used for multiple comparisons in FreeSurfer. P values for statistical significance after Monte Carlo simulation correction were a vertex-wise/cluster-forming threshold of 3 ($p < 0.001$) and a cluster-wise $P < 0.001$ (two-tailed). *Post hoc* multiple comparisons of cortical thickness were performed in SPSS and Bonferroni correction was used for *post hoc* multiple comparison corrections (adding age and education as covariates). MNI coordinates, Montreal Neurological Institute coordinates of the peak voxel. a: *P* values of *post hoc* multiple comparisons of cortical thicknesses among the CSVD-CI group, CSVD-no-CI group, and NC group

regions without altered ReHo may predict the onset of impaired global function in CSVD patients.

Specifically, the thickness of the right ACG was decreased only in the CSVD with CI group and not in the CSVD without CI group. Correlation analyses showed that both cortical thickness and ReHo in this region were significantly associated with memory function in CSVD with CI patients. The ACG is a subregion of the ventromedial frontal cortex, consisting of the cingulate sulcus and regions ventral to the superior frontal gyrus and dorsal to the corpus callosum[36]. Atrophy of the ACG has been reported in patients with asymptomatic lacunar infarcts[37] and the present study is the first to find cortical thinning in this region in CSVD patients. Although the ACG is mostly

involved in the regulation of executive function, emotional behavior, conflict, feedback, errors, and pain[36], increased ACG activation had been reported to be associated with the retrieval of episodic memory[38]. ACG infarction was also found to result in working memory dysfunction[39], in accordance with our finding that ACG regulated memory processes. However, correlation analyses revealed that higher ReHo values in the right ACG were associated with poorer memory function, including both short-term memory and long-term memory, in CSVD patients with CI. The higher local coherence of activity could be a sign of maladaptive brain activity and suggests functional deterioration in CSVD patients with CI[14]. In any case, decreased cortical thickness and normal ReHo in the right ACG may be of value in predicting the onset of CI in CSVD patients.

Importantly, although the CSVD without CI group retained normal global function, participants in this group exhibited impaired visuospatial function. In the present study, CI was defined according to performance in the MoCA test. The MoCA test has high sensitivity for CI and has been commonly used to detect CI in the previous studies[40,41]. However, our finding suggests that visuospatial function may have higher sensitivity for CI than the MoCA test in CSVD patients. Importantly, we also found that early impaired visuospatial function including visuospatial structure and visuospatial memory was associated with decreased cortical thickness of the right MTG in CSVD patients. Visuospatial function is an ability to comprehend visual representations and spatial relationships between objects and domains, including storage, retrieval, and transformation of spatial or visual stimuli[42]. Poor visuospatial attention had been found in

Table 5. Cortical thicknesses of the bilateral insula, right ACG, right cuneus, and right MTG among the CSVD-CI group, CSVD-no-CI group, and NC group

Brain region	Side	CSVD-CI group	CSVD-no-CI group	NC group
Insula	Left	2.32±0.19	2.42±0.19	2.54±0.18
Insula	Right	2.20±0.17	2.28±0.16	2.40±0.14
ACG	Right	2.37±0.17	2.50±0.16	2.53±0.17
Cuneus	Right	1.76±0.18	1.87±0.17	1.93±0.15
MTG	Right	2.17±0.30	2.28±0.29	2.48±0.27

Cortical thickness is reported in millimeters. Cortical thicknesses of brain regions are shown as mean±s.d.

Table 6. ReHo values of ROIs in the CSVD-CI group, CSVD-no-CI group, and NC group

Brain region	Side	CSVD-CI group	CSVD-no-CI group	NC group	*P*-value [a]	CSVD-CI group versus NC group [b]	CSVD-CI group versus CSVD-no-CI group[b]	CSVD-no-CI group versus NC group[b]
Insula	Left	-0.30±0.33	-0.40±0.24	-0.22±0.34	0.005	1.000	0.061	0.004
Insula	Right	-0.24±0.30	-0.26±0.25	-0.13±0.30	0.024	0.153	1.000	0.028
ACG	Right	0.07±0.30	0.15±0.27	0.09±0.27	0.266	1.000	0.333	0.752
Cuneus	Right	0.57±0.40	0.57±0.32	0.61±0.35	0.669	1.000	1.000	1.000
MTG	Right	-0.85±0.29	-0.84±0.31	-0.78±0.29	0.580	1.000	1.000	0.934

General linear model adjusted for age and education was used for ReHo analysis in SPSS among the CSVD-CI group, CSVD-no-CI group, and NC group. Bonferroni correction was used for *post hoc* multiple comparison corrections in general linear model. ReHo values of ROIs were shown as mean±s.d. [a]: *P* values of GLM analysis among the CSVD-CI group, CSVD-no-CI group, and NC group, [b]: *P* values of *post hoc* multiple comparisons of ReHo values among the CSVD-CI group, CSVD-no-CI group, and NC group

Table 7. Significant correlations between MRI parameters and cognitive scales

Group	Brain region	Cognitive scale	MRI parameter	Correlation coefficient	*P*-value
CSVD-CI group	Right ACG	AVLTIR	ReHo value	−0.369	0.002
CSVD-CI group	Right ACG	AVLTSTDR	ReHo value	−0.356	0.003
CSVD-CI group	Right ACG	AVLTLTDR	ReHo value	−0.372	0.002
CSVD-CI group	Right ACG	DSF	Cortical thickness	0.339	0.001
CSVD-no-CI group	Right MTG	BNT	Cortical thickness	0.327	0.015
CSVD-no-CI group	Right MTG	VRC	Cortical thickness	0.353	0.008
CSVD-no-CI group	Right MTG	VRIR	Cortical thickness	0.398	0.002
CSVD-no-CI group	Right MTG	VRDR	Cortical thickness	0.305	0.022

Partial correlation analysis was used to explore the association between the MRI parameters and cognitive scale scores, with age and education as covariates

asymptomatic CSVD patients whose neuropsychological tests were in the normal range[43] and we found that visuospatial structure and visuospatial memory dysfunction occurred before overall cognitive dysfunction. These findings suggest that visuospatial function may be the earliest impaired cognitive domain involved in CSVD. In addition, thinning of the right MTG may be the cause of visuospatial damage in CSVD patients whose overall cognition still maintained. Visual system studies have proposed that the ventral occipitotemporal and dorsal occipitoparietal pathways cooperate to convey the visual and spatial properties of the object[44] and the MTG serves as an important component[45]. Temporal cortex changes have also been found to be associated with visuospatial and visuoperceptual dysfunction in Parkinson's disease patients[46] and right parietotemporal gyrus atrophy was reported to be involved in visuospatial deficits in posterior cortical atrophy patients[47]. Thus, even if a CSVD patient exhibits normal global function (defined according to the MoCA test), assessing visuospatial function and cortical thickness in the right MTG are of great importance, potentially contributing to the detection of early CI in CSVD.

The previous studies have explored other features, including functional connectivity and the integrity of the WM tract, which are related to CI in CSVD patients[1,48]. However, conflicting results have been reported. This discrepancy may have resulted from differences in methodology between studies. For example, in analyses of functional connectivity, the selection of seed regions and methods for the identification of functional networks vary between studies[48]. Similarly, different methods have been employed to measure the integrity of the WM tract[1]. In contrast, our results are more consistent as the cortical thickness and ReHo are relatively easily measured on the basis of T1 images and BOLD images, respectively, and we used established methods to measure cortical thickness and ReHo. We took this approach to maximize the likelihood of our results having useful clinical applications, although more research will be required to validate the present findings in the future studies.

Brain functional alterations have traditionally been considered to occur earlier than structural alterations. However, our study found that the CSVD with the CI group exhibited decreased cortical thickness in five regions, but no altered ReHo, compared with the NC group. There are at least two possible reasons for this finding. First, the ReHo pattern was investigated in the mask of each region with decreased cortical thickness. Altered ReHo may occur in parts of each region or outside the five regions. Second, there may have been decreased and increased in ReHo in different regions, causing overall ReHo to remain unchanged. Nevertheless, we only explored the ReHo pattern in regions with decreased cortical thickness because we intended to focus on regions that exhibited stable structural changes. This may have helped to improve the stability and repeatability of results.

Several limitations of the present study should be considered. First, our study employed cross-sectional data and could not reveal causal effects of brain alterations on cognitive function. Longitudinal data would be helpful for detecting the causal relationships between brain alterations and cognitive function. Second, the CSVD with the CI group included both patients with MCI and those with dementia, but this differentiation was not taken into consideration, while the study explored the cortical thickness and ReHo of the participants. Future studies should focus on brain changes across different stages of CI in CSVD patients.

5. Conclusion

Decreased cortical thickness but normal ReHo in the right ACG, right cuneus, bilateral insula, and right MTG are characteristic changes related to the development of CI in CSVD patients, and impaired visuospatial function related to cortical thinning in the right MTG may provide a much earlier sign of CI in these patients. These findings shed light on potential markers related to CI in CSVD patients. Further research will be required to predict the onset of CI on the basis of these brain changes.

Acknowledgments

We thank all of the medical workers involved in this study for their contributions and all participants for taking part in this study.

Funding

This work was supported by the National Natural Science Foundation of China (81801060, 81971009).

Conflict of interest

The authors declare that they have no known conflicts of interest that could influence the work reported in this paper.

Author contributions

Conceptualization: Qing Ye and Xiaolei Zhu

Investigation: Xiaolei Zhu, Yuting Mo, Lili Huang, Ruomeng Qin, Zhihong Ke, Zheqi Hu, and Chenglu Mao

Formal analysis: Yuting Mo, Lili Huang, Kelei He, Biyun Xu, and Ruowen Qi

Writing – original draft: Yuting Mo and Lili Huang

Writing – review and editing: Qing Ye, Xiaolei Zhu, and Kelei He

References

1. Huang L, Chen X, Sun W, *et al*., 2020, Early segmental white matter fascicle microstructural damage predicts the corresponding cognitive domain impairment in cerebral small vessel disease patients by automated fiber quantification. *Front Aging Neurosci*, 12: 598242.

   https://doi.org/10.3389/fnagi.2020.598242

2. Cannistraro RJ, Badi M, Eidelman BH, *et al*., 2019, CNS small vessel disease: A clinical review. *Neurology*, 92(24): 1146–1156.

3. Jokinen H, Melkas S, Madureira S, *et al*., 2016, Cognitive reserve moderates long-term cognitive and functional outcome in cerebral small vessel disease. *J Neurol Neurosurg Psychiatry*, 87: 1296–1302.

   https://doi.org/10.1136/jnnp-2016-313914

4. Liu R, Wu W, Ye Q, *et al*., 2019, Distinctive and pervasive alterations of functional brain networks in cerebral small vessel disease with and without cognitive impairment. *Dement Geriatr Cogn Disord*, 47: 55–67.

   https://doi.org/10.1159/000496455

5. Chen H, Zhu H, Huang L, *et al*., 2022, The flexibility of cognitive reserve in regulating the frontoparietal control network and cognitive function in subjects with white matter hyperintensities. *Behav Brain Res*, 2022: 113831.

   https://doi.org/10.1016/j.bbr.2022.113831

6. Dey AK, Stamenova V, Turner G, *et al*., 2016, Pathoconnectomics of cognitive impairment in small vessel disease: A systematic review. *Alzheimers Dement*, 12: 831–845.

   https://doi.org/10.1016/j.jalz.2016.01.007

7. Chen H, Huang L, Yang D, *et al*., 2019, Nodal global efficiency in front-parietal lobe mediated periventricular white matter hyperintensity (PWMH)-related cognitive impairment. *Front Aging Neurosci*, 11: 347.

   https://doi.org/10.3389/fnagi.2019.00347

8. Banerjee G, Wilson D, Jager HR, *et al*., 2016, Novel imaging techniques in cerebral small vessel diseases and vascular cognitive impairment. *Biochim Biophys Acta*, 1862: 926–938.

   https://doi.org/10.1016/j.bbadis.2015.12.010

9. Lambert C, Narean JS, Benjamin P, *et al*., 2015, Characterising the grey matter correlates of leukoaraiosis in cerebral small vessel disease. *Neuroimage Clin*, 9: 194–205.

   https://doi.org/10.1016/j.nicl.2015.07.002

10. Li H, Jia X, Li Y, *et al*., 2021, Aberrant amplitude of low-frequency fluctuation and degree centrality within the default mode network in patients with vascular mild cognitive impairment. *Brain Sci*, 11: 1534.

    https://doi.org/10.3390/brainsci11111534

11. Wang Y, Yang Y, Wang T, *et al*., 2020, Correlation between white matter hyperintensities related gray matter volume and cognition in cerebral small vessel disease. *J Stroke Cerebrovasc Dis*, 29: 105275.

    https://doi.org/10.1016/j.jstrokecerebrovasdis.2020.105275

12. Tang J, Shi L, Zhao Q, *et al*., 2017, Coexisting cortical atrophy plays a crucial role in cognitive impairment in moderate to severe cerebral small vessel disease patients. *Discov Med*, 23: 175–182.

13. Zang Y, Jiang T, Lu Y, *et al*., 2004, Regional homogeneity approach to fMRI data analysis. *Neuroimage*, 22: 394–400.

    https://doi.org/10.1016/j.neuroimage.2003.12.030

14. Ye Q, Chen X, Qin R, *et al*., 2019, Enhanced regional homogeneity and functional connectivity in subjects with white matter hyperintensities and cognitive impairment. *Front Neurosci*, 13: 695.

    https://doi.org/10.3389/fnins.2019.00695

15. Prins ND, Scheltens P. White matter hyperintensities, cognitive impairment and dementia: An update. *Nat Rev Neurol*, 11: 157–165.

    https://doi.org/10.1038/nrneurol.2015.10

16. Wardlaw JM, Smith EE, Biessels GJ, *et al*., 2013, Neuroimaging standards for research into small vessel disease and its contribution to ageing and neurodegeneration. *Lancet Neurol*, 12:822–838.

    https://doi.org/10.1016/S1474-4422(13)70124-8

17. Lawrence AJ, Chung AW, Morris RG, *et al*., 2014, Structural network efficiency is associated with cognitive impairment in small-vessel disease. *Neurology*, 83: 304–311.

    https://doi.org/10.1212/WNL.0000000000000612

18. Lu J, Li D, Li F, *et al*., 2011, Montreal cognitive assessment in detecting cognitive impairment in Chinese elderly individuals: A population-based study. *J Geriatr Psychiatry Neurol*, 24: 184–190.

    https://doi.org/10.1177/0891988711422528

19. Fischl B, 2012, FreeSurfer. *Neuroimage*, 62: 774–781.

    https://doi.org/10.1016/j.neuroimage.2012.01.021

20. Sled JG, Zijdenbos AP, Evans AC, 1998, A nonparametric method for automatic correction of intensity nonuniformity in MRI data. *IEEE Trans Med Imaging*, 17: 87–97.

    https://doi.org/10.1109/42.668698

21. Dale AM, Fischl B, Sereno MI, 1999, Cortical surface-based analysis. I. Segmentation and surface reconstruction. *Neuroimage*, 9: 179–194.

https://doi.org/10.1006/nimg.1998.0395

22. Fischl B, Liu A, Dale AM, 2011, Automated manifold surgery: Constructing geometrically accurate and topologically correct models of the human cerebral cortex. *IEEE Trans Med Imaging*, 20: 70–80.

https://doi.org/10.1109/42.906426

23. Fischl B, Sereno MI, Dale AM, 1999, Cortical surface-based analysis. II: Inflation, flattening, and a surface-based coordinate system. *Neuroimage*, 9(2): 195–207.

https://doi.org/10.1006/nimg.1998.0396

24. Fischl B, Sereno MI, Tootell RB, *et al*., 1999, High-resolution intersubject averaging and a coordinate system for the cortical surface. *Hum Brain Mapp*, 8: 272–284.

https://doi.org/10.1002/(sici)1097-0193(1999)8:4<272::aid-hbm10>3.0.co;2-4

25. Fischl B, van der Kouwe A, Destrieux C, *et al*., 2004, Automatically parcellating the human cerebral cortex. *Cereb Cortex*, 14: 11–22.

https://doi.org/10.1093/cercor/bhg087

26. Desikan RS, Segonne F, Fischl B, *et al*., 2006, An automated labeling system for subdividing the human cerebral cortex on MRI scans into gyral based regions of interest. *Neuroimage*, 31: 968–980.

https://doi.org/10.1016/j.neuroimage.2006.01.021

27. Fischl B, Dale AM, 2000, Measuring the thickness of the human cerebral cortex from magnetic resonance images. *Proc Natl Acad Sci U S A*, 97: 11050–11055.

https://doi.org/10.1073/pnas.200033797

28. Klein A, Tourville J, 2012, 101 labeled brain images and a consistent human cortical labeling protocol. *Front Neurosci*, 6: 171.

https://doi.org/10.3389/fnins.2012.00171

29. Kloppenborg RP, Nederkoorn PJ, Geerlings MI, *et al*., 2014, Presence and progression of white matter hyperintensities and cognition: A meta-analysis. *Neurology*, 82: 2127–38.

https://doi.org/10.1212/WNL.0000000000000505

30. Alber J, Alladi S, Bae HJ, *et al*., 2019, White matter hyperintensities in vascular contributions to cognitive impairment and dementia (VCID): Knowledge gaps and opportunities. *Alzheimers Dement* (*NY*) 5: 107–117.

https://doi.org/10.1016/j.trci.2019.02.001

31. Brundel M, Kwa VI, Bouvy WH, *et al*., 2014, Cerebral microbleeds are not associated with long-term cognitive outcome in patients with transient ischemic attack or minor stroke. *Cerebrovasc Dis*, 37: 195–202.

https://doi.org/10.1159/000358119

32. Doi H, Inamizu S, Saito BY, *et al*., 2015, Analysis of cerebral lobar microbleeds and a decreased cerebral blood flow in a memory clinic setting. *Intern Med*, 54: 1027–1033.

https://doi.org/10.2169/internalmedicine.54.3747

33. Makin SD, Turpin S, Dennis MS, *et al*., 2013, Cognitive impairment after lacunar stroke: Systematic review and meta-analysis of incidence, prevalence and comparison with other stroke subtypes. *J Neurol Neurosurg Psychiatry*, 84: 893–900.

https://doi.org/10.1136/jnnp-2012-303645

34. Chen L, Song J, Cheng R, *et al*., 2020, Cortical thinning in the medial temporal lobe and precuneus is related to cognitive deficits in patients with subcortical ischemic vascular disease. *Front Aging Neurosci*, 12: 614833.

https://doi.org/10.3389/fnagi.2020.614833

35. Ni L, Liu R, Yin Z, *et al*., 2016, Aberrant spontaneous brain activity in patients with mild cognitive impairment and concomitant lacunar infarction: A resting-state functional MRI study. *J Alzheimers Dis*, 50: 1243–1254.

https://doi.org/10.3233/JAD-150622

36. Gasquoine PG, 2013, Localization of function in anterior cingulate cortex: from psychosurgery to functional neuroimaging. *Neurosci Biobehav Rev*, 37: 340–348.

https://doi.org/10.1016/j.neubiorev.2013.01.002

37. Chen Y, Wang J, Zhang J, *et al*., 2014, Aberrant functional networks connectivity and structural atrophy in silent lacunar infarcts: Relationship with cognitive impairments. *J Alzheimers Dis*, 42: 841–850.

https://doi.org/10.3233/JAD-140948

38. Cabeza R, Nyberg L, 2000, Imaging cognition II: An empirical review of 275 PET and fMRI studies. *J Cogn Neurosci*, 12: 1–47.

https://doi.org/10.1162/08989290051137585

39. Kobayashi Y, Morizumi T, Nagamatsu K, *et al*., 2021, Persistent working memory impairment associated with cerebral infarction in the anterior cingulate cortex: A case report and a literature review. *Intern Med*, 60: 3473–3476.

https://doi.org/10.2169/internalmedicine.6927-20

40. Abd Razak MA, Ahmad NA, Chan YY, *et al*., 2019, Validity of screening tools for dementia and mild cognitive impairment among the elderly in primary health care: A systematic review. *Public Health*, 169: 84–92.

https://doi.org/10.1016/j.puhe.2019.01.001

41. Zhuang L, Yang Y, Gao J, 2021, Cognitive assessment tools for mild cognitive impairment screening. *J Neurol*, 268: 1615–1622.

https://doi.org/10.1007/s00415-019-09506-7

42. Tallarita GM, Parente A, Giovagnoli AR, 2019, The visuospatial pattern of temporal lobe epilepsy. *Epilepsy Behav*, 101: 106582.

https://doi.org/10.1016/j.yebeh.2019.106582

43. Nie S, Shen C, Guo Y, *et al*., 2021, Preliminary findings on visual event-related potential P3 in asymptomatic patients with cerebral small vessel disease. *Neuropsychiatr Dis Treat*, 17: 3379–3394.

https://doi.org/10.2147/NDT.S338717

44. Farivar R, 2009, Dorsal-ventral integration in object recognition. *Brain Res Rev*, 61:144–153.

https://doi.org/10.1016/j.brainresrev.2009.05.006

45. Uithol S, Bryant KL, Toni I, *et al*., 2021, The anticipatory and task-driven nature of visual perception. *Cereb Cortex*, 31: 5354–5362.

46. Ibarretxe-Bilbao N, Junque C, Marti MJ, *et al*., 2011, Brain structural MRI correlates of cognitive dysfunctions in Parkinson's disease. *J Neurol Sci*, 310: 70–74.

https://doi.org/10.1016/j.jns.2011.07.054

47. Andrade K, Kas A, Valabrègue R, *et al*., 2012, Visuospatial deficits in posterior cortical atrophy: Structural and functional correlates. *J Neurol Neurosurg Psychiatry*, 83: 860–863.

https://doi.org/10.1136/jnnp-2012-302278

48. Schulz M, Malherbe C, Cheng B, *et al*., 2021, Functional connectivity changes in cerebral small vessel disease a systematic review of the resting-state MRI literature. *BMC Med*, 19: 103.

https://doi.org/10.1186/s12916-021-01962-1